Received: 27 April 2023 | Revised: 12 September 2023 | Accepted: 19 September 2023

DOI: 10.1002/mgg3.2288

Molecular Genetics & Genomic Medicine Open Access WILEY

CLINICAL REPORT

Defective C3d caused by *C3* p.W1034R in inherited atypical hemolytic uremic syndrome

Masafumi Tsuchida[1] | **Shin Goto**[1] | **Hirofumi Watanabe**[1] | **Sawako Goto**[2] | **Hiroki Yamaguchi**[1] | **Ichiei Narita**[1]

[1]Division of Clinical Nephrology and Rheumatology, Kidney Research Center, Niigata University Graduate School of Medical and Dental Sciences, Niigata, Japan

[2]Department of Applied Molecular Medicine, Kidney Research Center, Niigata University Graduate School of Medical and Dental Sciences, Niigata, Japan

Correspondence
Shin Goto, Division of Clinical Nephrology and Rheumatology, Kidney Research Center, Niigata University Graduate School of Medical and Dental Sciences, 1-757, Asahimachi-dori, Chuou-ku, Niigata City, Niigata, Japan.
Email: gotos@med.niigata-u.ac.jp

Funding information
Grant-in-Aid for Scientific Research B, Grant/Award Number: 19H03674; Grant-in-Aid for Scientific Research C, Grant/Award Number: 15K09250

Abstract

Introduction: Atypical hemolytic uremic syndrome (aHUS) is a rare form of thrombotic microangiopathy. Personal genome analyses have revealed numerous aHUS-causing variants, mainly complement-related genes. However, not all aHUS-causing variants have been functionally validated.

Methods: An exome sequence analysis of a Japanese multiplex family composed of three patients diagnosed with aHUS in infancy and showing frequent relapses clustered in a dominant transmission mode was performed. Protein interaction between the C3d and C-terminal domains of factor H was analyzed using a quartz crystal microbalance.

Results: Following filtering by heterozygous variants, amino acid substitutions, and allele frequency, the analysis revealed eight rare variants shared by the affected individuals. Variant prioritization listed *C3* p.W1034R as the most likely candidate gene mutation in the affected individuals, despite being classified as a variant of uncertain significance. Binding of recombinant C3d harboring 1034R to recombinant short consensus repeats 15 to 20 of factor H was significantly suppressed compared with that of C3 with 1034W.

Conclusion: *C3* p.W1034R results in an inherited form of aHUS that often presents with recurrent episodes, possibly because of impaired interactions between the C3d and C-terminal domains of factor H. Following comprehensive genomic analysis, functional validation of C3 p.W1034R strengthens the molecular basis for aHUS pathophysiology.

KEYWORDS
atypical hemolytic uremic syndrome, C3d mutation, complement C3, exome sequence, quartz crystal microbalance

1 | INTRODUCTION

Hemolytic uremic syndrome (HUS) features microangiopathic hemolytic anemia, thrombocytopenia, and renal impairment, with symptoms similar to those of thrombotic thrombocytopenic purpura (Noris & Remuzzi, 2009). Approximately 10% of HUS cases are classified as atypical because of the absence of Shiga toxin-producing

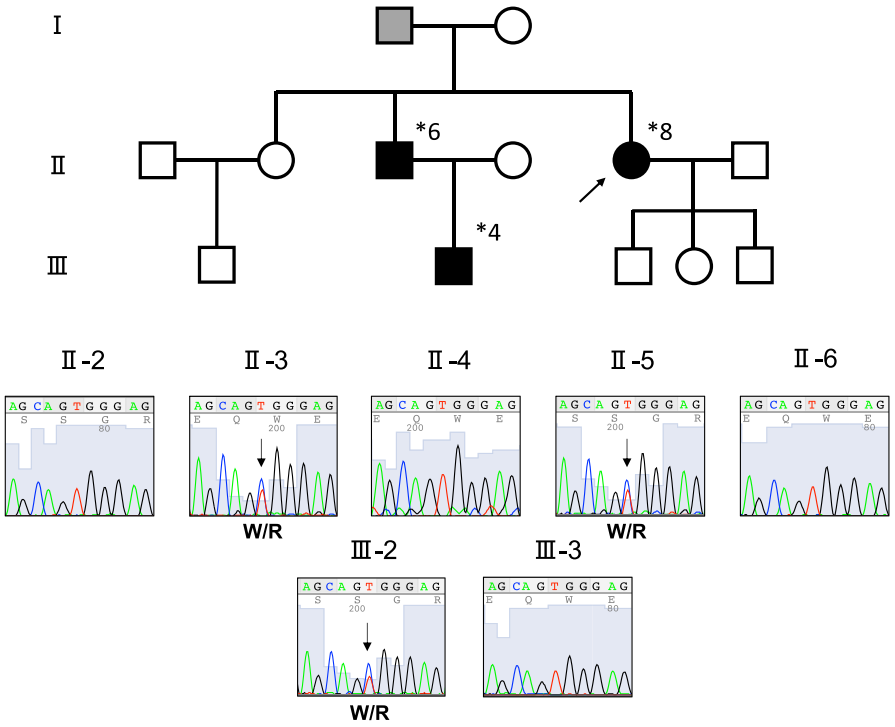

FIGURE 1 Pedigree of the family in this study and Sanger sequence of *C3* c.3100. (a) Pedigree of a family with atypical hemolytic uremic syndrome (aHUS). Black, white and gray denote affected individuals, unaffected individuals, and individuals suspected of having aHUS, respectively. The arrow represents the index case. * suggests the number of relapses in the clinical course. (b) Sanger sequence of *C3* c.3100. The affected individuals have heterozygous *C3* c.3100T>C (arrow) leading to amino-acid substitution of tryptophan to arginine (W/R), whereas the unaffected individuals have no variant in this allele.

bacterial infections or other known triggers (Noris & Remuzzi, 2009). Atypical HUS (aHUS; OMIM: #235400) is caused by abnormalities of the alternative complement system, with a poor prognosis and high mortality rate, with up to 10% of patients dying and 50% of the patients progressing to end-stage renal disease (Noris & Remuzzi, 2009).

Approximately 50% of aHUS cases are caused by genetic abnormalities (Noris & Remuzzi, 2009), especially complement-regulating gene abnormalities. Comprehensive genomic analysis has revealed numerous variants associated with aHUS (Bu et al., 2018); however, functional validation is necessary to confirm the causative variants for each aHUS phenotype. Herein, we report findings of whole exome and protein interaction analyses of three patients with aHUS from one family.

2 | MATERIALS AND METHODS

2.1 | Informed consent

Informed consent and assent were obtained from all participants or their parents.

2.2 | Whole-exome sequencing

Whole-exome sequencing was performed on an Ion Proton™ Sequencer using the Ion PI™ Sequencing 200 kit v3 (both from Thermo Fisher Scientific, Waltham, MA) (Figure 1). The sequenced reads were processed using Torrent Suite™ Software v4.0.2, on the Ion Torrent Server. Reads were mapped against the human reference genome hg19 using the Torrent Mapping Alignment Program. Torrent Variant Caller v5.0.7 detected variants and generated variant call format (VCF) files, which were processed and annotated using Ion Reporter™ Software v5.2.

2.3 | Filtering and prioritization of genetic variants

The variants were filtered to include heterozygous and nonsynonymous or splicing variants and shared by all three affected patients (Wang et al., 2010). Variants with allele frequencies >0.01 in the East Asian population were excluded in gnomAD (The Genome Aggregation Database). Phenotype-based variant prioritization (Zhao et al., 2020) in each affected individual was assessed, in addition to the candidate genes, according to the guidelines published in 2015 by the American College of Medical Genetics and Genomics (ACMG) and the Association for Molecular Pathology (AMP; Li & Wang, 2017).

2.4 | Recombinant C3d

As *C3* p.W1034R was considered the most probable candidate variant for a causative mutation in this family with aHUS (Zhao et al., 2020; Table S1), a functional

analysis was conducted using a recombinant glutathione S-transferase (GST)-tagged C3 protein in which the amino acid at the 1034 position was substituted with arginine to demonstrate the functional effects of the variant (Supplementary Methods). Briefly, the PCR-amplified fragments of *C3* from 3004 to 3909 (Figure 2a), corresponding to C3d, were inserted into the pGEX6P-1 vector (Cytiva, Tokyo, Japan), and the recombinant GST-tagged C3d protein was expressed and purified using a glutathione Sepharose 4B column (Cytiva, Tokyo, Japan). Subsequently, the GST tag was removed by overnight incubation with PreScission Protease (Cytiva, Tokyo, Japan) at 4°C. A 3100T>C mutation in *C3d* introduced into the pGEX6P-1 vector was induced using a mutagenesis kit (Toyobo, Osaka, Japan). As controls that had been reported to have deleterious effects on the binding between C3b protein and factor H (Schramm et al., 2015), the vectors harboring the 3187 A > C mutation, which leads to an amino-acid substitution of serine to arginine (S1063R), and the 3281 C > A mutation, which leads to an amino-acid substitution of alanine to aspartate (A1094D), were also constructed.

2.5 | Interaction between C3d and factor H

The interaction between factor H and recombinant C3d was evaluated using a quartz crystal microbalance (QCM) affinity biosensor (AFFINIX Q8; ULVAC, Inc., Kanagawa, Japan). Briefly, 2.5 μg of each recombinant C3d with p.1034W, p.1034R, or controls (p. S1063R and p. A1094D) was immobilized on a sensor chip using the

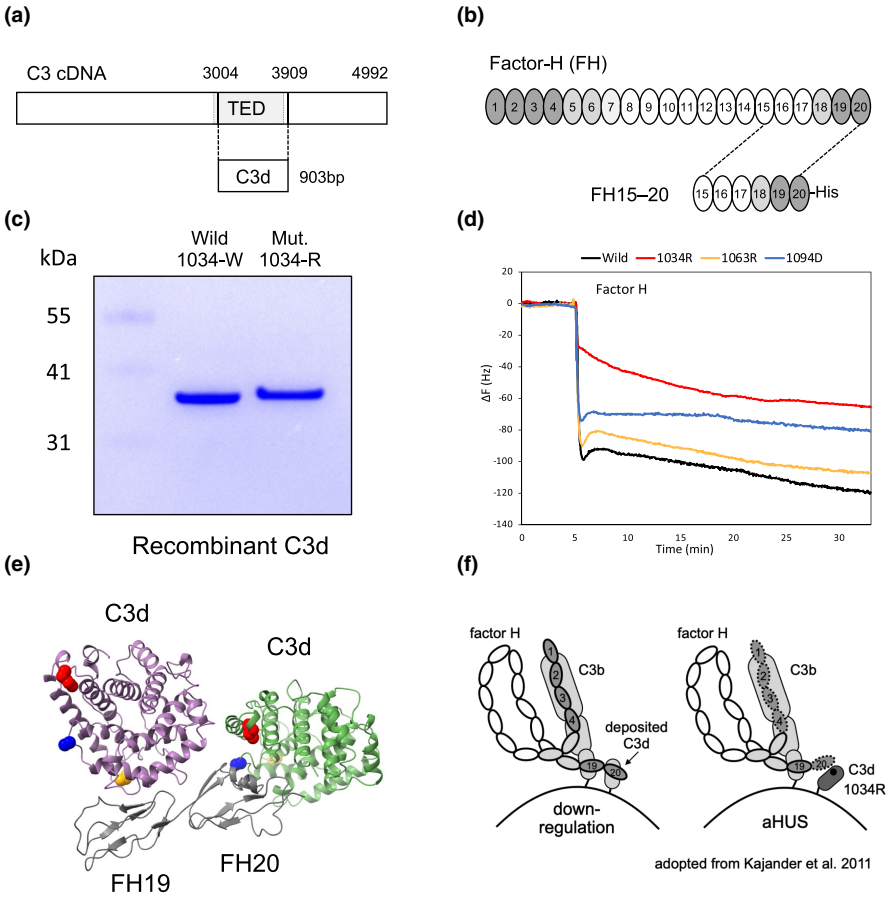

FIGURE 2 Binding between C3d and FH15–20. (a) Construction, expression, and purification of C3d. 903 bp of C3d cDNA (3004–3909 in C3 cDNA) was cloned into the GST tag vector. (b) Short consensus repeats 15–20 of factor H (FH15-20). (c) Coomassie brilliant blue staining of recombinant C3d of wild type (Wild, 1034-W) and mutation type (Mut., 1034-R) showed 34 kDa proteins. (d) Quartz crystal microbalance analysis was used to monitor the binding curve between recombinant C3d and factor H of short consensus repeats 15–20. Black lines denote the wild type of C3d (1034W), red lines denote 1034R, yellow lines denote 1063R, and blue lines denote 1094D. The arrow represents the time at which factor H was injected. (e) Molecular structure of a complex composed of C3d and FH19–20. Red denotes tryptophan at the 1034 amino acid position, blue denotes serine at the 1063 amino acid position, and yellow denotes alanine at the 1094 amino acid position of the C3 protein. (f) Model of regulation of the C3 amplification loop (based on Kajander et al., 2011). FH20 binds to deposited C3d (left) and reduces the binding of FH20 to C3d-1034R, resulting in dysregulation of the C3 amplification loop (right).

amine coupling method, as previously reported (Hori et al., 2017). Thereafter, 2.0 μg of recombinant human factor H comprising short consensus repeats 15–20 (FH15–20, R&D Systems, Minneapolis, MN) was injected into the chamber in a buffer containing 200 μL of 10 mM HEPES, 150 mM NaCl, and 2 mM $CaCl_2$, at pH 7.4. The interaction curve was monitored for approximately 40 min. The average data obtained using two sensors were evaluated under each condition.

2.6 | Visualization of a complex composed of C3d and FH19–20

Structural data regarding complexes composed of C3d and FH19–20 (Protein database [PDB] ID: 2XQW) were downloaded from PDB and visualized with UCSF ChimeraX software (version 1.6rc202304180021; Pettersen et al., 2021).

3 | RESULTS

3.1 | Clinical phenotype of the family with aHUS

The pedigree of the aHUS patients is shown in Figure 1. A 24-year-old patient (II-5, index case) was diagnosed with aHUS at infancy and experienced recurrent thrombotic angiopathic symptoms, including hemolytic anemia, thrombocytopenia, and kidney failure. Her laboratory data on admission showed a red blood cell count of $365\times10^4/mm^3$, 11.0 g/dL hemoglobin, $1.6\times10^4/mm^3$ platelet, 26.6 mg/dL urea nitrogen, 0.70 mg/dL creatinine, 1761 IU/L lactate dehydrogenase, 3.68 mg/dL total bilirubin, and a negative result for the Coombs test. ADAMTS13 activity was 42%, and the antibody against ADAMTS13 was negative. The serum level of complement C3 was 97 mg/dL. Urinary test showed 3+ for protein and occult blood. Considering a history of frequent relapses, she was diagnosed with aHUS relapse. Subsequently, she was treated with a pulse steroid and administered fresh frozen plasma. Thereafter, her platelet count, LDH, and bilirubin levels returned to within the normal range. Her brother and his son were also diagnosed with aHUS based on renal biopsy findings. Despite experiencing multiple episodes of aHUS—six episodes in the patient, four in her brother, and two in her nephew—kidney function was preserved in all.

3.2 | Whole exome sequencing and prioritization of candidate gene

Approximately 50,000–60,000 variants per individual were identified. First, we selected heterozygous variants that caused amino acid substitutions and filtered them to obtain 1854 variants shared by the affected individuals. Sixty-seven variants were not found in unaffected individuals. Eight variants had a minor allele frequency of <0.1% in the East Asian population with gnomAD (Figure S1A, Table 1). Among them, *C3* c.3100T>C, which results in the most damaging score of amino acid substitutions with p.Trp1034Arg, has not been reported in the Japanese Reference Genome Sequence. Additionally, phenotype-based gene prioritization listed *C3* as the most likely candidate variant for aHUS in all affected individuals (Table S1). In both II-3 and III-2, *DGKE* was listed as the second candidate gene; *DGKE* p.W285L has not been reported in any genomic reference database. However, this *DGKE* variant was heterozygous, and unaffected individuals in the family also had the variant; therefore, we considered this to be a noncausative variant.

Sanger sequencing confirmed the cosegregation of *C3* c.3100T>C within this family (Figure 1), suggesting that

TABLE 1 Candidate variants selected by filtering whole-exome sequence data.

Chr	Type	Gene	Protein	Coding	gnomAD	JRGS	dbSNP	Sift	Polyphen2
2	SNV	*OR6B3*	p.Val74Met	c.220G>A	0.00022	0.008	rs201073756	0.002	0.992
4	SNV	*TBC1D14*	p.Pro296Arg	c.887C>G	NA	0.0012	rs997523629	0.081	0.984
5	SNV	*ANKRD31*	p.Gln1825Glu	c.5473C>G	NA	0.0019	rs149690398	0.333	
5	SNV	*POLK*	p.Ala471Val	c.1412C>T	0.0009	0.0012	rs149894654	0.004	0.999
19	SNV	*BSG*	p.His86Arg	c.257A>G	0.0008	0.0023	rs185020271	0.882	0
19	SNV	*C3*	p.Trp1034Arg	c.3100T>C	NA	NA	NA	0.000	0.994
19	SNV	*ZNF534*	p.Thr642Ala	c.1924A>G	NA	0.0054	rs148845163	0.022	0.24
19	SNV	*LILRB2*	p.Ala391Val	c.1172C>T	0.0008	0.0066	rs201242685	0.086	0.166

Abbreviations: Chr, chromosome; gnomAD, the Genome Aggregation Database; JRGA, Japanese Reference Genome Sequence; NA, not applicable; SNV, single nucleotide variant.

it is mostly a disease-causing variant. According to the ACMG/AMP 2015 guidelines, *C3* p.W1034R is a variant of uncertain significance, owing to its absence in control populations.

3.3 | Recombinant C3d

The purity of the GST-tagged C3d protein exceeded 95%, with a molecular weight of 60 kDa (Figure S1B). PreScission Protease was added to GST-tagged C3d bound to the Sepharose 4B column, releasing the GST-tag-free C3d protein with a molecular weight of 34 kDa (Figure S1B, Figure 2c). Figure 2b shows the recombinant human FH15–20 used.

3.4 | Binding between C3d and factor H

In the QCM analysis, frequency changes indicated the binding of the guest protein to each protein immobilized on the sensor. After guest protein injection, the sensor immobilized with C3d-1034W showed a steep drop in significant frequency, whereas the sensor with immobilized C3d-1034R significantly suppressed frequency change (Figure 2d). Subsequently, parallel curves were obtained for both proteins. Control proteins (C3d-1063R and C3d-1094D) showed suppressed frequency change with each pattern between 1034W and 1034R.

4 | DISCUSSION

Our analysis revealed that the most probable candidate genetic variant is *C3* p.W1034R in aHUS patients aggregated with the family, despite *C3* p.W1034R being interpreted as a variant of uncertain significance (Li & Wang, 2017). Recombinant C3d protein comprising the variant of tryptophan to arginine at the 1034 amino-acid position exhibited less affinity with the C-terminal domain of factor H; therefore, the mutated C3d protein could functionally affect the C3 amplification loop in the alternative pathway.

Numerous gene variants, particularly complement-regulating gene variants, in aHUS have been identified using genetic analysis (Bu et al., 2014, 2018; Fremeaux-Bacchi et al., 2008; Schramm et al., 2015). Notably, not all variants in these genes are clinically pathogenic; therefore, discriminating pathogenic from nonpathogenic variations is necessary to determine the causative variants (Bu et al., 2018). Here, we prioritized *C3* p.W1034R from the variants obtained by exome sequencing. Although the ACMG/ASP guidelines interpret *C3* p.W1034R as a variant of uncertain significance, the European aHUS registry has three aHUS cases harboring heterozygous p.W1034R (Schramm et al., 2015). We found the same variant inherited in an autosomal fashion, indicating that *C3* p.W1034R can cause familial aHUS with childhood-onset and repeated relapses despite the functional validation needed.

Here, the binding of C3d-1034R to FH15–20 was significantly lower than that of C3d-1034W. In a previous study that analyzed the functional effects of C3 protein by its gene mutations from the European aHUS registry (Schramm et al., 2015), *C3* p.W1034R had a negligible effect on the affinity between C3b and complement regulatory proteins, including factor H. However, *C3* p.W1034R could exert its effects in other ways. Structural molecular analysis (Kajander et al., 2011) revealed that the C-terminal of factor H has two binding sites: C3d part of the C3 protein, SCR 19 (FH19), and SCR 20 (FH20). Factor H regulates C3 activation through the binding of FH19 to the C3d part of C3b, and the FH20 glycosaminoglycan binding site to polyanions of host cells. Additionally, factor H is assumed to regulate the feedback loop of C3 amplification by binding FH20 to C3d deposited and broken down from C3b in host cells (Kajander et al., 2011). The binding sites of C3d to FH19 or FH20 are reported to be different (Kajander et al., 2011). Considering p.W1034R resides near FH20 binding sites (Figure 2e), C3d-1034R might affect the binding between C3d and FH20. Conversely, the degree of binding change in C3d variants in the present study could be mainly attributed to the change in the folding of each protein. We inferred less binding between C3d and FH20, resulting in the dysregulation of the C3 amplification loop (Figure 2f), although it might be possible that *C3* p.W1034R significantly exerts influences on the entire C3 protein. It should be kept in mind that understanding genotype–phenotype association is essential for understanding the roles of detected variants in the context of aHUS pathophysiology.

A nationwide epidemiological survey of 118 patients reported that the frequency of *C3* mutations in patients with aHUS in Japan is 27.1% (Fujisawa et al., 2018). In the thioester domain (TED), p.R1042L, p.K1105Q, and p.I1157T have been described as *C3* mutations in Japanese patients with aHUS, whereas p.W1034R has not been reported. Patients with *C3* p.I1157T have higher relapse rates but better outcomes than those with other *C3* mutations (Fujisawa et al., 2018). Similar to those with p.I1157T, patients with p.W1034R show relatively modest disease courses, despite frequent relapses, particularly during childhood. Considering the similar phenotype, there may be a common underlying pathophysiology among patients with aHUS harboring mutations in the TED domain.

The limitation of this study is that the results revealed by our genomic analysis were not demonstrated by clinical samples such as the sera of the patients. The study included only three members of a single family; therefore, further studies are required to obtain high-level evidence regarding *C3* p.W1034R as a causative mutation of aHUS.

5 | CONCLUSIONS

Whole exome and protein binding analyses revealed *C3* p.W1034R as a causative mutation of aHUS in the family included in this study. Defective C3d, degraded from C3b, could have a pathogenic role in developing aHUS with a less severe outcome but repeated relapse.

AUTHOR CONTRIBUTIONS

Masafumi Tsuchida: genomic data analysis, recombinant C3d experiment and binding analysis, and manuscript writing. Shin Goto: study design, genomic data analysis, recombinant C3d experiment, and manuscript writing. Hirofumi Watanabe: genomic data analysis and manuscript writing. Sawako Goto: QCM binding analysis and manuscript writing. Hiroki Yamaguchi: recombinant C3d experiment and QCM binding analysis. Ichiei Narita: manuscript editing. All authors approved the final manuscript.

ACKNOWLEDGMENTS

The authors thank Dr. Hajime Yamazaki from Nagaoka Red Cross Hospital, Dr. Yoshihiko Hidaka from Shinshu University, and Dr. Toshio Watanabe from Gunma University for their contribution to sample collection. A part of this study was presented at the Annual Meeting of the American Society of Nephrology, Kidney Week 2016. This work was supported by a Grant-in-Aid for Scientific Research B (no. 19H03674 to I. Narita) and a Grant-in-Aid for Scientific Research C (no. 15K09250 to S. Goto) from the Ministry of Education, Culture, Sports, and Technology of Japan. We would like to thank Editage (www.editage.com) for English language editing.

CONFLICT OF INTEREST STATEMENT

None to declare.

DATA AVAILABILITY STATEMENT

The data are not publicly available because of ethical restrictions.

ETHICS STATEMENT

This study was approved by the Ethics Committee on Genetic Analysis of Niigata University, Niigata, Japan (approval no. G2015-0510, G2017-0007, and G2021-0035) and conducted according to the principles of the Declaration of Helsinki.

ORCID

Shin Goto https://orcid.org/0000-0002-6167-555X

REFERENCES

Bu, F., Maga, T., Meyer, N. C., Wang, K., Thomas, C. P., Nester, C. M., & Smith, R. J. (2014). Comprehensive genetic analysis of complement and coagulation genes in atypical hemolytic uremic syndrome. *Journal of the American Society of Nephrology*, *25*(1), 55–64. https://doi.org/10.1681/ASN.2013050453

Bu, F., Zhang, Y., Wang, K., Borsa, N. G., Jones, M. B., Taylor, A. O., Takanami, E., Meyer, N. C., Frees, K., Thomas, C. P., & Smith, R. J. H. (2018). Genetic analysis of 400 patients refines understanding and implicates a new gene in atypical hemolytic uremic syndrome. *Journal of the American Society of Nephrology*, *29*(12), 2809–2819. https://doi.org/10.1681/ASN.2018070759

Fremeaux-Bacchi, V., Miller, E. C., Liszewski, M. K., Strain, L., Blouin, J., Brown, A. L., Moghal, N., Kaplan, B. S., Weiss, R. A., Lhotta, K., Kapur, G., Mattoo, T., Nivet, H., Wong, W., Gie, S., Hurault de Ligny, B., Fischbach, M., Gupta, R., Hauhart, R., … Atkinson, J. P. (2008). Mutations in complement C3 predispose to development of atypical hemolytic uremic syndrome. *Blood*, *112*(13), 4948–4952. https://doi.org/10.1182/blood-2008-01-133702

Fujisawa, M., Kato, H., Yoshida, Y., Usui, T., Takata, M., Fujimoto, M., Wada, H., Uchida, Y., Kokame, K., Matsumoto, M., & Nangaku, M. (2018). Clinical characteristics and genetic backgrounds of Japanese patients with atypical hemolytic uremic syndrome. *Clinical and Experimental Nephrology*, *22*(5), 1088–1099. https://doi.org/10.1007/s10157-018-1549-3

Hori, Y., Aoki, N., Kuwahara, S., Hosojima, M., Kaseda, R., Goto, S., Iida, T., De, S., Kabasawa, H., Kaneko, R., & Saito, A. (2017). Megalin blockade with cilastatin suppresses drug-induced nephrotoxicity. *Journal of the American Society of Nephrology*, *28*(6), 1783–1791. https://doi.org/10.1681/ASN.2016060606

Kajander, T., Lehtinen, M. J., Hyvarinen, S., Bhattacharjee, A., Leung, E., Isenman, D. E., Meri, S., Goldman, A., & Jokiranta, T. S. (2011). Dual interaction of factor H with C3d and glycosaminoglycans in host-nonhost discrimination by complement. *Proceedings of the National Academy of Sciences of the United States of America*, *108*(7), 2897–2902. https://doi.org/10.1073/pnas.1017087108

Li, Q., & Wang, K. (2017). InterVar: Clinical interpretation of genetic variants by the 2015 ACMG-AMP guidelines. *American Journal of Human Genetics*, *100*(2), 267–280. https://doi.org/10.1016/j.ajhg.2017.01.004

Noris, M., & Remuzzi, G. (2009). Atypical hemolytic-uremic syndrome. *The New England Journal of Medicine*, *361*(17), 1676–1687. https://doi.org/10.1056/NEJMra0902814

Pettersen, E. F., Goddard, T. D., Huang, C. C., Meng, E. C., Couch, G. S., Croll, T. I., Morris, J. H., & Ferrin, T. E. (2021). UCSF ChimeraX: Structure visualization for researchers, educators, and developers. *Protein Science*, *30*(1), 70–82. https://doi.org/10.1002/pro.3943

Schramm, E. C., Roumenina, L. T., Rybkine, T., Chauvet, S., Vieira-Martins, P., Hue, C., Maga, T., Valoti, E., Wilson, V., Jokiranta,

S., Smith, R. J., Noris, M., Goodship, T., Atkinson, J. P., & Fremeaux-Bacchi, V. (2015). Mapping interactions between complement C3 and regulators using mutations in atypical hemolytic uremic syndrome. *Blood*, *125*(15), 2359–2369. https://doi.org/10.1182/blood-2014-10-609073

Wang, K., Li, M., & Hakonarson, H. (2010). ANNOVAR: Functional annotation of genetic variants from high-throughput sequencing data. *Nucleic Acids Research*, *38*(16), e164. https://doi.org/10.1093/nar/gkq603

Zhao, M., Havrilla, J. M., Fang, L., Chen, Y., Peng, J., Liu, C., Wu, C., Sarmady, M., Botas, P., Isla, J., Lyon, G. J., Weng, C., & Wang, K. (2020). Phen2Gene: Rapid phenotype-driven gene prioritization for rare diseases. *NAR Genomics and Bioinformatics*, *2*(2), lqaa032. https://doi.org/10.1093/nargab/lqaa032

SUPPORTING INFORMATION

Additional supporting information can be found online in the Supporting Information section at the end of this article.

How to cite this article: Tsuchida, M., Goto, S., Watanabe, H., Goto, S., Yamaguchi, H., & Narita, I. (2024). Defective C3d caused by *C3* p.W1034R in inherited atypical hemolytic uremic syndrome *Molecular Genetics & Genomic Medicine*, *12*, e2288. https://doi.org/10.1002/mgg3.2288